Colin P. Derdeyn, MD
Tom O. Videen, PhD
Nicholas R. Simmons, BA
Kent D. Yundt, MD
Susanne M. Fritsch, RN
Robert L. Grubb, Jr, MD
William J. Powers, MD

Index terms:
Brain, emission CT (ECT), 10.12163
Brain, ischemia, 10.781
Carotid arteries, stenosis or obstruction, 172.721, 175.721
Emission CT (ECT), experimental studies, 10.12163

Radiology 1999; 212:499–506

Abbreviations:
OEF = oxygen extraction fraction
ROC = receiver operating characteristic
STLCOS = St Louis Carotid Occlusion Study

[1] From the Section of Neuroradiology (C.P.D.) and Div of Radiological Sciences (C.P.D., T.O.V., N.R.S., R.L.G., W.J.P.), Mallinckrodt Institute; Dept of Neurology and Neurological Surgery (T.O.V., K.D.Y., S.M.F., R.L.G., W.J.P.); and Lillian Strauss Institute of the Jewish Hospital of St Louis (W.J.P.), Washington University School of Medicine, 510 S Kingshighway Blvd, St Louis, MO 63110. From the 1998 RSNA scientific assembly. Received Sep 16, 1998; revision requested Nov 17; revision received Dec 7; accepted Mar 2, 1999. Supported by National Institutes of Health grants NS02029 (C.P.D.), NS28947 (T.O.V., S.M.F., R.L.G., W.J.P.), and NS34050 (W.J.P.) and Charles A. Dana Foundation (C.P.D., K.D.Y., W.J.P.) and by RSNA Research and Education Foundation as a 1994 Siemens Medical Systems/RSNA Fellow (C.P.D.). Address reprint requests to C.P.D. (e-mail: *derdeyn@mirlink.wustl.edu*).

Author contributions:
Guarantor of integrity of entire study, C.P.D.; study concepts and design, W.J.P., C.P.D.; definition of intellectual content, W.J.P., C.P.D.; literature research, C.P.D., W.J.P.; clinical studies, W.J.P., R.L.G., C.P.D., S.M.F., K.D.Y.; experimental studies, C.P.D., W.J.P., T.O.V.; data acquisition, C.P.D., S.M.F., K.D.Y., W.J.P., R.L.G., T.O.V.; data analysis, C.P.D., W.J.P., T.O.V., N.R.S.; statistical analysis, C.P.D., W.J.P.; manuscript preparation, C.P.D.; manuscript editing, W.J.P.; manuscript review, W.J.P., R.L.G., T.O.V.

Count-based PET Method for Predicting Ischemic Stroke in Patients with Symptomatic Carotid Arterial Occlusion[1]

PURPOSE: To test the ability of a count-based positron emission tomographic (PET) method, without arterial sampling, for the measurement of regional cerebral oxygen extraction fraction (OEF) to predict ischemic stroke in patients with symptomatic carotid arterial occlusion.

MATERIALS AND METHODS: The outcome analysis of a blinded prospective study designed to determine if increased OEF was an independent predictor of stroke in patients with symptoms and with carotid occlusion was repeated by substituting a count-based method of OEF measurement for the original quantitative technique. The performance of the quantitative and count-based methods was assessed by using Kaplan-Meier cumulative survival functions (log-rank, [$P < .05$]). Receiver operating characteristic (ROC) curves for both methods were generated.

RESULTS: Thirteen ipsilateral strokes occurred during a mean follow-up of 3.1 years for 81 patients. All ipsilateral strokes occurred in 50 patients with increased count-based OEF ($P = .002$, sensitivity 100%, specificity 46%). Sixty-eight patients underwent complete quantitative studies, which allowed comparison of OEF methods. Both the count-based and the quantitative methods were predictive of stroke in this subgroup ($P = .005$ and .025, respectively). ROC analysis demonstrated a greater area under the curve for the count-based OEF method.

CONCLUSION: Count-based PET measurement of OEF without arterial sampling accurately predicts stroke in patients with carotid occlusion.

The hemodynamic effect of ipsilateral carotid arterial occlusion has been categorized into three stages (1). The rationale for this scheme is based on the known compensatory responses made by the cerebrovasculature to progressive reductions in cerebral perfusion pressure. When cerebral perfusion pressure is normal (stage 0), cerebral blood flow is closely matched to the resting metabolic rate of the tissue. As a consequence of this resting balance between flow and metabolism, the oxygen extraction fraction (OEF) shows little regional variation. Moderate reductions in cerebral perfusion pressure have little effect on cerebral blood flow. Dilatation of arterioles reduces cerebrovascular resistance, thus maintaining a constant blood flow (stage 1). This phenomenon is known as cerebrovascular autoregulation.

With more severe reductions in cerebral perfusion pressure, the capacity for compensatory vasodilation is exceeded, and cerebral blood flow begins to decline (Fig 1). A progressive increase in OEF then maintains cerebral oxygen metabolism and brain function (stage 2, Fig 1). This most severe form of cerebral hemodynamic failure also has been termed "misery perfusion" (2). At present, OEF can be measured only with PET and oxygen 15–labeled radiotracers.

Severe atherosclerotic disease of the carotid and vertebral arteries or their intracranial branches can lead to reduced perfusion pressure in the distal cerebral circulation, which depends primarily on the adequacy of collateral sources of blood flow (3). While the relative role of hemodynamic factors in the pathogenesis of ischemic stroke has become a moot question for patients with carotid stenosis, it remains an important issue for many patients with cerebrovascular disease, particularly those with occlusion of the carotid artery

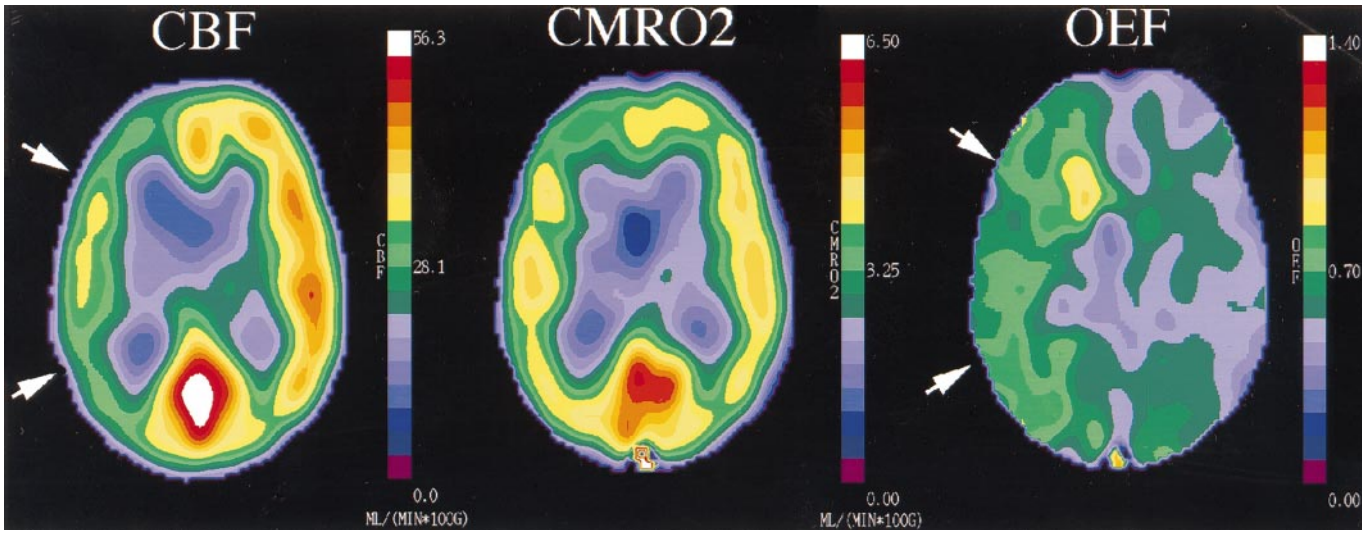

Figure 1. Positron emission tomographic (PET) scans show increased OEF, or "misery perfusion." This patient was 65 years old when he enrolled in the STLCOS after several transient ischemic attacks involving his right leg. His first symptoms occurred approximately 4 months prior to enrollment and PET examination. A CT scan at the time of the PET study demonstrated a small lacunar infarction of the right internal capsule. Neurologic examination results were normal. Cerebral angiography revealed an occlusion of the left internal carotid artery. The quantitative map of cerebral blood flow (*CBF*) on the far left demonstrates diffuse decrease in flow throughout the left cerebral hemisphere (arrows; note that left and right are reversed on these PET images relative to CT and MR conventions). The image depicting cerebral metabolic rate of oxygen consumption (*CMRO2*) in the middle shows normal and symmetric metabolism of oxygen. The quantitative OEF image on the far right shows increased OEF in the left hemisphere (arrows). The ability of the brain to increase the fraction of oxygen extracted from the blood allows normal oxygen metabolism and neurologic function, once the capacity for autoregulatory vasodilation has been exceeded and blood flow begins to decrease. This patient was treated with aspirin and had a fatal ipsilateral ischemic stroke 525 days after enrollment.

(4). Up to 15% of patients presenting with symptoms of acute cerebral or ocular ischemia have occlusion of the ipsilateral carotid artery (5–7). Their annual risk for subsequent stroke is 5%–7% (8). The presence of hemodynamic compromise long has been suspected as a factor in the pathogenesis of recurrent ischemic stroke in these patients, but without conclusive proof (3,4,9–11).

Findings of the St Louis Carotid Occlusion Study (STLCOS) recently demonstrated that increased OEF was an independent predictor of subsequent stroke in patients with symptomatic carotid occlusion in a blinded longitudinal study (12). In PET studies in patients with carotid occlusion before and after extracranial-to-intracranial arterial bypass, the OEF elevation has been shown to be reversible (2,13–15). Consequently, a clinical trial of surgical revascularization for patients with increased OEF has been proposed (12).

The quantitative measurement of an in vivo physiologic process, such as cerebral OEF, with PET is complicated (16). Three basic components are necessary: (*a*) a radiotracer, (*b*) a radiation detection system, and (*c*) a mathematic model relating the physiologic process to the detected radiation. For the quantitative measurement of OEF, a subject first inhales trace amounts of ^{15}O-labeled oxygen mixed with air. The ^{15}O-labeled oxygen is then bound to hemoglobin and transported throughout the body where some of it is used for oxidative metabolism. Some ^{15}O-labeled oxygen is metabolized to water, which returns to the bloodstream and recirculates.

As these processes are occurring, the ^{15}O radionuclides are decaying by emission of a positron. These positively charged particles can travel a few millimeters within a tissue before encountering an electron. This interaction leads to annihilation of both the positron and the electron and generates two photons of equal energy heading in opposite directions. The PET scanner uses data from detector pairs to create an image of regional activity, or PET counts, and this PET image of regional counts must be processed to translate regional activity to a physiologic measurement.

The quantitative measurement of OEF requires time-activity data acquired from arterial sampling during scanning and quantitative values of blood flow and blood volume provided from separate PET examinations (17). This information is used to correct for the PET counts measured in the head owing to unextracted ^{15}O-labeled oxygen, which remains bound to hemoglobin, and the PET counts from recirculating ^{15}O-labeled water owing to metabolism of ^{15}O-labeled oxygen.

Metabolic processing of PET images is complicated and time-consuming. Percutaneous arterial cannulation may not be possible in some patients. Arterial sampling requires additional equipment and adds time to the PET procedure. In the STLCOS, complete arterial time-activity data were not available owing to technical factors in 13 of 81 subjects. These 13 subjects were therefore assigned to categories on the basis of the count-based method of OEF measurement presented in this report, while the remaining 68 subjects were assigned to categories by using the quantitative OEF processing. A count-based technique that does not require arterial time-activity data would be useful, particularly in the setting of a multiinstitutional trial in which standardization of complicated quantitative PET techniques might be difficult.

In this article, we present a further evaluation of the count-based PET technique to measure relative OEF (Fig 2). The count-based OEF image is generated by dividing the PET counts in an ^{15}O-labeled oxygen scan by the PET counts in an ^{15}O-labeled water scan on a pixel-by-pixel basis. The ratio of the counts in the ^{15}O-labeled oxygen image and the ^{15}O-labeled water image are linearly propor-

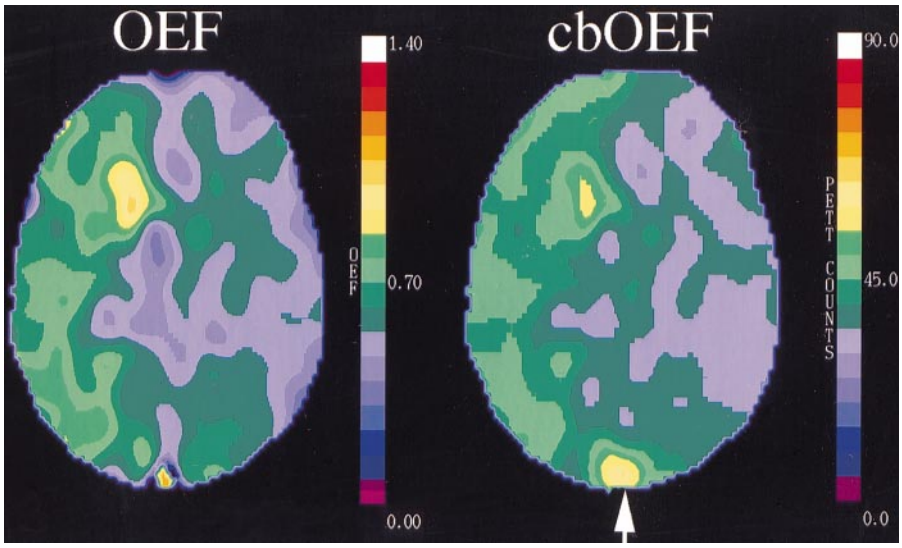

Figure 2. PET scans show the similarity of quantitative (on the left) and count-based (on the right) OEF images in the same patient as in Figure 1. The image on the right is the count-based oxygen extraction (*cbOEF*) image, which was generated by dividing the ^{15}O-labeled oxygen image by the ^{15}O-labeled water image. With the exception of the sagittal sinus (arrow on the *cbOEF* image), the regional map of oxygen extraction is very similar to that of the quantitative OEF image on the left. As the count-based OEF image is not corrected for intravascular ^{15}O-labeled oxygen, the sagittal sinus has more activity than on the quantitatively processed OEF image. High values of OEF can be seen in the center of the sagittal sinus on the quantitative OEF image, which may be owing to misregistration of the cerebral blood volume scan during processing.

tional to quantitative regional OEF except for the small contributions from intravascular oxygen and recirculating labeled water. The errors are small when regional oxygen metabolism is normal (17–19).

In the present study, we compared the results of repeating the outcome analysis of the STLCOS by using both the count-based method and the quantitative method of OEF measurement. The purpose of this study was to evaluate the accuracy of the count-based OEF method to predict ischemic stroke in patients with symptomatic carotid arterial occlusion.

MATERIALS AND METHODS

Patients and Control Subjects

Eighty-one patients with symptomatic unilateral atherosclerotic carotid arterial occlusion were enrolled in the STLCOS, a blinded prospective study of cerebral hemodynamics and ischemic stroke. The study was designed to test the hypothesis that increased OEF measured in the cerebral hemisphere distal to the occluded carotid artery was an independent predictor of stroke in these patients. Enrollment began in 1992 and ended in 1996. Analysis of both the baseline risk factors and of the long-term follow-up of these patients has been published (12,20). Details of the study design, patient population, and inclusion and exclusion criteria can be found in these two reports.

Patients were followed-up by the study coordinator (S.M.F.) for the duration of the study by telephone contact every 6 months with the patient or next of kin. The occurrence of any symptoms suggesting a stroke was thoroughly evaluated by one designated investigator (R.L.G.), who remained blinded to the PET data. All living patients were followed-up for the duration of the study. The primary end point of the original prospective study was subsequent ischemic stroke defined clinically as a neurologic deficit of presumed ischemic cerebrovascular cause lasting more than 24 hours in any cerebrovascular territory. Secondary end points were ipsilateral ischemic stroke and death.

Eighteen healthy control subjects (eight women, 10 men; age range, 19–77 years; mean age ± SD, 45 years ± 18) were recruited by means of public advertisement. All underwent neurologic evaluation, magnetic resonance (MR) imaging of the head, and duplex ultrasonographic (US) imaging of the extracranial carotid arteries. None had (*a*) signs or symptoms of neurologic disease other than mild distal sensory loss in the legs consistent with age, (*b*) pathologic lesions on MR images (mild atrophy and punctate asymptomatic white matter abnormalities were not considered pathologic), or (*c*) more than 50% stenosis of the extracranial carotid arteries.

A computed tomographic (CT) scan of the brain was obtained without contrast enhancement if CT or MR imaging had not been performed as part of the usual clinical care sufficiently long after an ischemic event to permit accurate definition of infarction location. This CT scan was used to determine the site of tissue infarction to exclude these regions from subsequent PET analysis.

This research was approved by the human studies committee and written informed consent was obtained from all subjects.

PET Examination

Hemodynamic PET studies in patients with carotid occlusion were performed at study entry. Blood pressure was measured in the clinic prior to walking to the scanner suite. After positioning the patient in the scanner gantry, an individually molded thermoplastic face mask was applied to ensure that the patient's head remained in a constant position during the scanning period. The exact position of the patient's head relative to the scanning plane was recorded on a lateral skull radiograph obtained after head immobilization. Venous and, when possible, arterial catheters were placed for the intravenous administration of the radiotracer and for arterial blood gas analyses and arterial time-activity curve determination, respectively (21). All PET studies were performed with use of one of two scanners (ECAT 953B or ECAT EACT HR; Siemens/CTI, Knoxville, Tenn). A transmission scan was obtained by using the two-dimensional mode (intersection septa extended) before radiotracer administration by using germanium 68/gallium 68 rotating rod sources.

Each PET study consisted of three separate physiologic studies. During each, arterial blood samples were drawn by hand or automatically to convert quantitative regional radioactivity data to quantitative physiologic measurements. Additional arterial samples were drawn at intervals during the examination for determination of $Paco_2$ stability, mean arterial oxygen content calculations, and carboxyhemoglobin content.

A 5-minute scan was obtained 1 minute and 45 seconds after inhalation of one to two breaths of air containing trace amounts of ^{15}O-labeled carbon monox-

ide. After allowing this activity to decay for approximately 15 minutes, a 40-second scan was obtained after inhalation of one to two breaths of air containing trace amounts of ^{15}O-labeled oxygen. After another 15 minutes, the last scan was acquired after the injection of a bolus of ^{15}O-labeled water.

Both the ^{15}O-labeled oxygen scans and ^{15}O-labeled water scans acquired counts for 40 seconds, beginning when the radiotracer reached the brain. The circulation time for intravenously administered or inhaled radiotracer to reach the brain varies greatly from person to person, so accurate online monitoring of brain radioactivity is necessary to start data acquisition at the proper time. Both scanners used in this study provide such online monitoring of coincidence events within the field of view, but the temporal resolution is poor unless data acquisition is underway.

Another potential problem is that there is a delay after scan initiation before data are acquired. This delay does not occur during advancement from one dynamic frame of data acquisition to another, however. Thus, it was necessary to modify the scan acquisition protocols to include two dynamic frames: Frame 1 had no preset duration and was begun 5–10 seconds prior to radiotracer administration. Frame 2 was preset to be 40 seconds in duration and was begun by the scanner operator when the coincidence events in the field of view sharply increased and indicated the arrival of the radiotracer bolus in the brain. Only the data from frame 2 was reconstructed and used in subsequent analysis.

The entire PET examination could be performed within 1 hour because of the short half-life (122.2 seconds) of ^{15}O. All radionuclides were produced in the Washington University cyclotron facility (22,23).

Image Processing and Analysis

All images were reconstructed by using filtered backprojection and scatter correction with a ramp filter at the Nyquist frequency. They were then filtered with a three-dimensional Gaussian filter to a uniform resolution of 16 mm full width at half maximum. These images subsequently were transformed to stereotactic atlas space (24) by using the lateral skull radiograph and the transmission scan. This was done to allow reproducible placement of regions of interest.

When combined with the arterial time-activity curve data and the hematocrit values, the ^{15}O-labeled carbon monoxide image provided the quantitative regional measurement of cerebral blood volume on a pixel-by-pixel basis (25). A regional map of quantitative cerebral blood flow was generated from the ^{15}O-labeled water image by using arterial time-activity data (21,26,27). The ^{15}O-labeled oxygen image provided the quantitative regional measurement of OEF, once combined with data from processed cerebral blood flow and cerebral blood volume images and the arterial time-activity curve information (17). Images depicting cerebral metabolic rate for oxygen were generated as the product of OEF, cerebral blood flow, and Pa_{O_2} content (17).

The count-based OEF image was generated as the ratio image of the counts in the filtered and atlas-transformed ^{15}O-labeled oxygen and ^{15}O-labeled water images, normalized to a whole-brain mean of 0.40—this value was the mean whole-brain quantitative OEF measured in the 68 patients with arterial time-activity curve data. This was performed in the following manner.

First, the normalization factor was calculated: (*a*) A template was created by using brain edges defined by isointensity contours at approximately 30% of the whole-brain maximum counts of the ^{15}O-labeled water image to eliminate extracranial noise—the water image was used rather than the oxygen image because of the greater number of counts (ie, less noise); (*b*) this template was saved and used to mask the extracranial noise in the ^{15}O-labeled oxygen image; (*c*) whole-section mean counts for 21 PET sections that included the middle cerebral arterial territories were calculated from both the ^{15}O-labeled water and ^{15}O-labeled oxygen scans by using the saved templates to mask the extracranial noise; (*d*) the ratio of the ^{15}O-labeled oxygen counts to the ^{15}O-labeled water counts was calculated; and (*e*) 0.40 was divided by this ratio to yield the normalization factor (0.40 = normalization factor × [whole-brain ^{15}O-labeled oxygen counts/whole-brain ^{15}O-labeled water counts]).

Next, a second mask was created in a similar manner to eliminate extracranial noise from the ^{15}O-labeled oxygen images and ^{15}O-labeled water images prior to the pixel-by-pixel division of the counts in the images: (*a*) A mask image was created from the ^{15}O-labeled water image by using the same threshold percentage used for the template in the calculation of the normalization factor and in an identical manner (brain edges identified by means of isointensity contours at a specified threshold percentage of maximum whole-brain counts), and (*b*) this mask was applied to the ^{15}O-labeled oxygen image.

Finally, the counts in the masked ^{15}O-labeled oxygen image were multiplied by the normalization factor and divided by the counts in the masked ^{15}O-labeled water image on a pixel-by-pixel basis. This resulted in the count-based OEF image used in the subsequent regional analyses (Fig 2).

For each patient and healthy volunteer, seven separate spherical regions of interest 19 mm in diameter were placed in the territory of the middle cerebral artery in each hemisphere. Each region included gray and white matter and was placed by using stereotactic coordinates (1,28). Areas of prior infarction were identified by two investigators (C.P.D., W.J.P.) by review of images depicting cerebral metabolic rate for oxygen (or ^{15}O-labeled images for the 13 patients without arterial data) and CT or MR images. Neither the regions within these areas nor the corresponding contralateral regions were used for analysis. Left-to-right ratios of mean hemispheric values of both quantitative OEF images and count-based OEF images were calculated for patients and control subjects. For each patient, the ratio was considered abnormal if it decreased beyond the range observed in the normal sample.

Data Analysis

Several analyses were performed. First, the ability of the count-based OEF ratio to predict subsequent stroke was examined. The 81 patients were divided into two groups on the basis of comparison with the range of normal values: those with abnormal count-based OEF ratios and those with normal count-based OEF ratios. The primary analysis compared the two groups with respect to the length of time before reaching the end point of ipsilateral stroke by means of Kaplan-Meier survival curves and the log-rank statistic.

Second, the count-based technique was compared directly with the quantitative method in predicting ipsilateral stroke. In these analyses, the image data of the 68 patients with arterial time-activity curves was processed by using both count-based and quantitative methods. Quantitative and count-based OEF ratios were compared for each patient by means of a paired Student *t* test.

Finally, receiver operating characteristic (ROC) curves for the prediction of subsequent ischemic stroke were generated by varying the threshold ratio used for a positive test for both quantitative and count-based techniques. This was

done by progressively increasing the threshold for an abnormal test result from a left-to-right OEF ratio of 1.00 ± 0.01 (0.99 to 1.01) to 1.00 ± 0.28 (0.72 to 1.28) by increments of 0.01. A value of $P < .05$ was used as the criterion of statistical significance. Statistical analyses were performed with SPSS 7.0 (SPSS, Chicago, Ill) for Windows.

RESULTS

Clinical

Eighty-one patients were followed up for a mean of 3.1 years. All patients had unilateral carotid occlusion. Fifteen strokes were recorded during the follow-up period, and all of them were ischemic. Thirteen of these strokes were ipsilateral to the occluded carotid artery.

Normal Range

The range for left-to-right hemispheric ratios for the quantitative OEF observed in the 18 healthy subjects was 0.914–1.084. The normal range of left-to-right hemispheric ratios for count-based OEF was 0.935–1.062 in these subjects.

Results of Count-based OEF for All 81 Patients

Fifty of the 81 patients with symptomatic carotid occlusion had abnormal results, with left-to-right hemispheric count-based ratios that fell outside of the range observed in the healthy subjects. In all 50, the hemisphere with the increased count-based OEF was ipsilateral to the occluded carotid artery. All 13 ipsilateral ischemic strokes occurred in the 50 patients with an increased count-based OEF ($P = .002$). The sensitivity of the count-based method for the prediction of subsequent ipsilateral stroke was 100% (95% CI = −23%) (29) with use of the range observed in the healthy subjects to define the normal range. However, 37 of the 68 patients who did not have an ipsilateral stroke had increased OEF (specificity of 46% [95% CI: 40.5%, 51.5%]). The Kaplan-Meier cumulative failure curve is shown in Figure 3. The ROC curve generated by progressively increasing the threshold at which the count-based OEF ratio was defined as abnormal is shown in Figure 4.

Comparison of Count-based and Quantitative Methods

Complete quantitative metabolic processing of PET images could not be performed for 13 of the 81 patients. Difficulty with arterial access or with the measurement of arterial blood counts during the PET examination accounted for 11 of these 13 studies. Arterial access could not be established in six: Four patients were taking warfarin sodium (Coumadin; Du Pont Pharma, Wilmington, Del) and failed Allen tests bilaterally, and in two patients several attempts at both radial and brachial arterial catheterization failed. Technical problems related to the quantitative processing of PET data accounted for the remaining seven patients. These problems involved malfunctioning of the device used to measure the arterial blood counts automatically in five patients.

Nine ipsilateral strokes occurred in the 68 patients with complete quantitative data. By using the normal range of values observed in the healthy volunteers to define the threshold, 31 of the 68 patients had abnormal results with use of quantitative OEF ratios. Seven ipsilateral ischemic strokes occurred in this group of 31 patients, compared with two strokes in the 37 patients with quantitative OEF ratios within the normal range ($P = .025$; sensitivity of 78% [95% CI: 64.5%, 91.5%]; specificity of 59% [95% CI: 52.2%, 65.8%]). The count-based OEF ratio was less specific (specificity of 48% [95% CI: 41.2%, 54.8%]) and more sensitive (sensitivity of 100% [95% CI = −33%]) than the quantitative method. Forty-one patients had abnormal results, and all strokes occurred in this group ($P = .005$). Kaplan-Meier cumulative failure curves of the quantitative and count-based analyses for these 68 patients are shown in Figure 5a and 5b, respectively.

Comparison of the count-based OEF ratio with the quantitative OEF ratio for each of the 68 patients demonstrated no significant difference at paired Student t test analysis ($P = .299$). The mean absolute difference between count-based OEF and quantitative OEF ratios was 0.034 (95% CI: 0.025, 0.043). ROC curves were generated for both methods (Fig 6). The area under the curve for the count-based OEF method (0.815) was greater than that for the quantitative OEF method (0.737).

DISCUSSION

In this retrospective analysis of STLCOS data, we have demonstrated that the count-based measurement of OEF can be used to identify patients at increased risk of ischemic stroke with accuracy similar to that of the quantitative method. By using the count-based OEF ratio instead of the quantitative OEF ratio for all 81 patients, we found that all 13 subsequent ipsilateral strokes occurred in the 50 patients with abnormal ratios. When the Kaplan-Meier survival functions of the two OEF processing methods were compared directly in the 68 patients with complete quantitative data, both achieved statistical significance. Direct comparison of count-based and quantitative OEF ratios showed no statistical difference (mean absolute difference = 0.034; 95% CI: 0.025, 0.043).

Why does the count-based method presented in this article perform as well as, if not better than, the quantitative OEF technique in the prediction of subsequent stroke? The data from the count-based OEF image are linearly proportional to the quantitative OEF image except for the small contributions from intravascular oxygen and recirculating labeled water.

The equation for quantitative OEF developed by Mintun et al (17) is as follows:

$$\begin{aligned}\mathrm{OEF} = [\mathrm{PET}_{\mathrm{obs}} - \mathrm{CBF} &\times \int_{t1}^{t2} C_{\mathrm{art}}^{\mathrm{H_2O}}(t) * e^{-kt}\,dt - R \times \mathrm{CBV} \\ &\times \int_{t1}^{t2} C_{\mathrm{art}}^{\mathrm{O_2}}(t)\,dt] \div [\mathrm{CBF} \\ &\times \int_{t1}^{t2} C_{\mathrm{art}}^{\mathrm{O_2}}(t) * e^{-kt}\,dt - (0.835) \\ &\times R \times \mathrm{CBV} \int_{t1}^{t2} C_{\mathrm{art}}^{\mathrm{O_2}}(t)\,dt].\end{aligned}$$

$\mathrm{PET}_{\mathrm{obs}}$ is the regional, decay-corrected PET counts measured in the brain after inhalation of a bolus of ^{15}O-labeled oxygen summed over a 40-second scan; obs is "observed." CBF × $\int_{t1}^{t2} C_{\mathrm{art}}^{\mathrm{H20}}(t) * e^{-kt}dt$ is the activity due to the recirculating labeled water owing to ^{15}O-labeled oxygen metabolism, where CBF is cerebral blood flow, $t1$ and $t2$ are the scanning time, and $C_{\mathrm{art}}^{\mathrm{H20}}$ is the time-dependent concentration of ^{15}O-labeled water in the arterial blood. The term $R \times \mathrm{CBV} \times \int_{t1}^{t2} C_{\mathrm{art}}^{\mathrm{O2}}(t)dt$ defines the post midcapillary activity of the intravascular ^{15}O-labeled oxygen where R is the ratio of small-vessel to large-vessel hematocrit values used in the calculation of CBV, CBV is the cerebral blood volume, and $C_{\mathrm{art}}^{\mathrm{O2}}$ is the time-dependent concentration of ^{15}O-labeled oxygen in the arterial blood.

The two terms in the denominator of the equation are the blood flow delivering the oxygen (CBF × $\int_{t1}^{t2} C_{\mathrm{art}}^{\mathrm{O2}}[t] * e^{-kt}dt$) minus the intravascular ^{15}O-labeled oxygen ($0.835 \times R \times \mathrm{CBV} \int_{t1}^{t2} C_{\mathrm{art}}^{\mathrm{O2}}[t]dt$). This method requires separate measurements

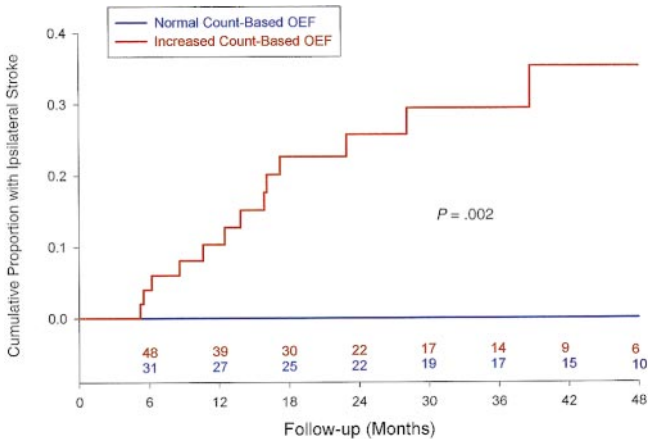

Figure 3. Graph shows Kaplan-Meier cumulative failure curves for the end point of ipsilateral stroke for all 81 patients with symptomatic carotid occlusion who were examined by using the count-based OEF method. None of the patients with normal count-based OEF ratios had an ipsilateral stroke (blue line). All 13 ipsilateral strokes occurred in the 50 patients with increased OEF (red line). The number of patients remaining event free and available for follow-up evaluation at each 6-month interval is shown at the bottom of the graph. The numbers in blue correspond to patients with normal OEF and the numbers in red to those with increased OEF. The vertical axis shows the cumulative proportion of patients with ipsilateral stroke. The difference in outcome was highly statistically significant.

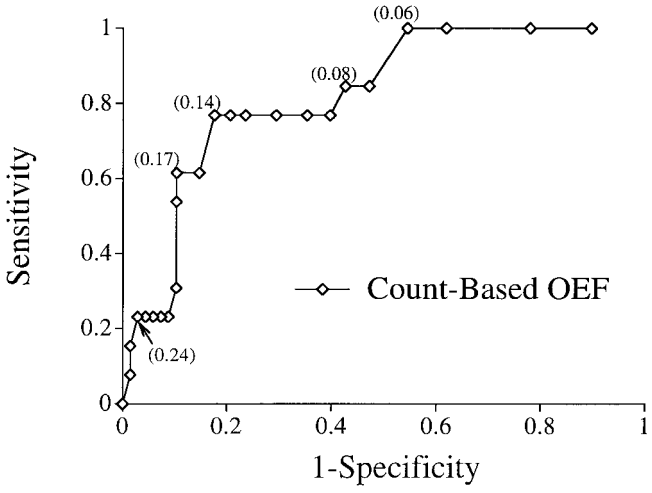

Figure 4. Graph shows ROC curve for the count-based OEF method for all 81 patients. Sensitivities and specificities of the count-based OEF ratio for the prediction of ipsilateral stroke were calculated at progressively larger thresholds from 1.00 ± 0.01 (0.99–1.01) to 1.00 ± 0.28 (0.72–1.28) by increments of 0.01. Several of these thresholds are indicated in parentheses next to their corresponding points on the curve. At threshold ratios up to 1.06 (in parentheses as 0.06, fourth point from the right), all subsequent ipsilateral strokes occur in the patients who have abnormal OEF ratios. However, the specificity of the count-based method at these thresholds is very low, as nearly all patients are considered to have abnormal OEF ratios. As specificity improves (moving to the left on the curve), sensitivity begins to decrease.

of cerebral blood flow and cerebral blood volume to yield an accurate quantitative measurement of OEF. It has been validated in nonhuman primates by using intracarotid injections of ^{15}O-labeled oxygen (17). In addition, it has been rigorously validated in nonhuman primates against direct measurements of arteriovenous oxygen difference in pathologic conditions (30).

The contribution of the recirculating labeled water of metabolism and the intravascular labeled oxygen to the counts measured in the brain is small in areas of normal cerebral oxygen metabolism (discussed later). Without these terms, the equation for OEF becomes the observed PET counts from the ^{15}O-labeled oxygen image divided by the cerebral blood flow delivering the oxygen.

In the tissue autoradiographic technique of blood flow measurement used in our laboratory, the relationship between the tissue concentration of ^{15}O-labeled water to the local blood flow is almost linear (21,26). In the count-based OEF method, therefore, we use the regional PET counts observed during the ^{15}O-labeled oxygen scanning for the numerator and the regional PET counts observed during the ^{15}O-labeled water scanning for the denominator: count-based OEF = PET_{obs} (^{15}O-labeled oxygen)/PET_{obs} (^{15}O-labeled water). Because we are comparing the ratio of the counts from the ^{15}O-labeled oxygen images and the counts from the ^{15}O-labeled water images from one hemisphere to the other, rather than using the absolute values for comparison between patients, the left-to-right ratio for the count-based estimate of OEF should be very similar to the left-to-right ratio of quantitative OEF.

In the first PET methods for OEF measurement, the ratio of counts from a steady-state or equilibrium ^{15}O-labeled oxygen image to a steady-state ^{15}O-labeled water image was used. This method was proposed by Jones and co-workers (31) before implementation and validation by Frackowiak et al (32). In this technique, blood flow is measured by using a continuous inhalation of ^{15}O-labeled carbon dioxide. The labeled carbon dioxide is converted to labeled water by carbonic anhydrase in the lung and enters the blood. A steady-state situation in which the delivery of labeled water to the brain becomes equal to the washout and decay of tracer is reached after several half-lives.

The measured activity in the brain at this point is directly proportional to the blood flow. Quantitative values are provided by converting PET counts to milliliters per gram per minute by means of an arterial sample for the measurement of activity in the blood. A similar steady-state scan is obtained during the continuous inhalation of ^{15}O-labeled oxygen. The ratio of the counts obtained during the oxygen scan to the counts measured during the water scan is linearly proportional to the OEF, except for the contribution of intravascular activity.

Baron and co-workers (18) compared the results of the steady-state ^{15}O PET technique, uncorrected for intravascular ^{15}O, with direct measurements of arteriovenous oxygen differences while changing $Paco_2$ in baboons. They found a linear relationship between the measured PET OEF and the arteriovenous oxygen difference. A consistent 13.3% overestimation of OEF by PET was found: OEF (arteriovenous oxygen difference) = 1.009 OEF (PET) + 13.3 ($P < .001$). To our knowledge, the first published description of misery perfusion used this uncorrected count-based technique of OEF measurement (2). In subsequent steady-state PET studies (19,33) that incorporated a correction for the intravascular ^{15}O-labeled oxygen, the mean percentage of overestimation of actual quantitative OEF in uninfarcted tissue by using the uncorrected count-based method was 11%–14% in gray matter and 8%–9% in white matter.

The ROC analysis demonstrates similar

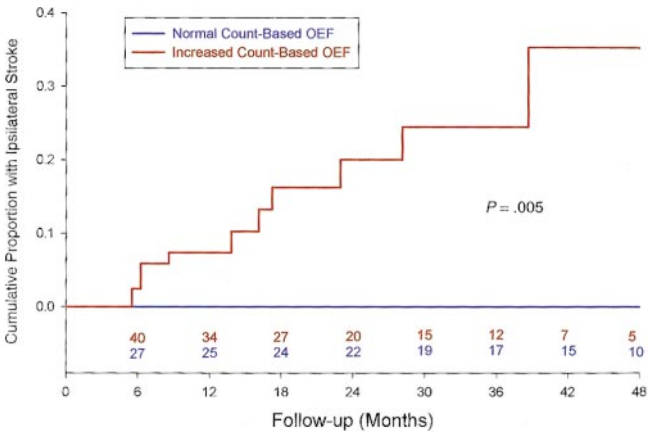

a.

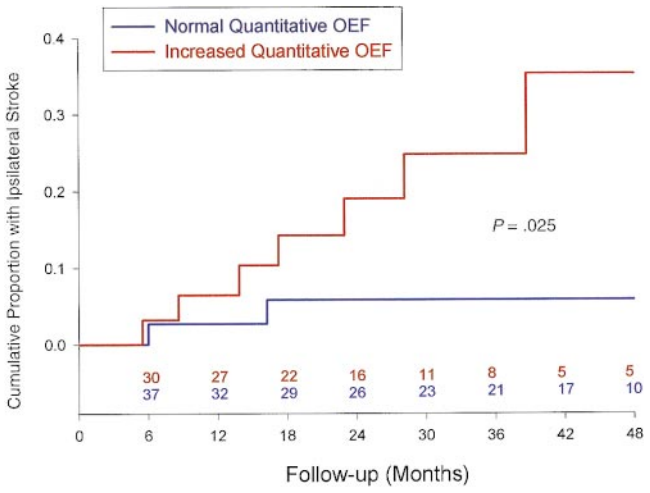

b.

Figure 5. Graphs show Kaplan-Meier cumulative failure curves for the 68 patients with complete quantitative data allowing comparison of count-based OEF and quantitative OEF methods. **(a)** Graph demonstrates the results for count-based OEF. **(b)** Graph shows the results for quantitative OEF. The vertical axis shows the cumulative proportion of patients with ipsilateral stroke. The numbers above the time intervals indicate the total number of patients remaining for follow-up at each 6-month period. The numbers in blue correspond to patients with normal OEF and the numbers in red to those with increased OEF. While the difference in outcome remains statistically significant for both techniques in this smaller group of patients, by using the threshold range of normal OEF established in the healthy volunteers the count-based method is 100% sensitive (all nine ipsilateral strokes occurred in the 41 patients with abnormal OEF), while the quantitative OEF method is not (two strokes occurred in the 37 patients with OEF inside the normal range). Fewer patients have abnormal OEF with the quantitative technique, however (31 compared with 41).

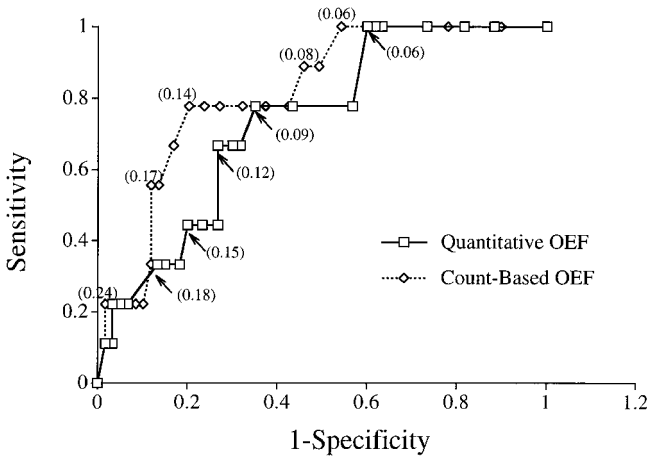

Figure 6. Graph shows ROC curves for the count-based (dotted line) compared with the quantitative (solid line) methods of OEF processing for the 68 patients with complete quantitative data. Sensitivities and specificities of both methods for the prediction of ipsilateral stroke were calculated at progressively greater thresholds from left-to-right ratios of 1.00 ± 0.01 (0.99–1.01) to 1.00 ± 0.28 (0.72–1.28) by increments of 0.01. Several of these thresholds are indicated in parentheses next to their corresponding points on the curve. Higher values of both sensitivity and specificity are seen with the count-based method compared with those of the quantitative technique at nearly all points along the curve. However, owing to the small number of strokes, it is not possible to determine if this apparent improvement in accuracy is real.

sensitivity and specificity of the quantitative and count-based methods. In fact, the area under the curve is greater with the count-based technique. Thus, the count-based method performs as well as, if not better than, the quantitative technique in the prediction of subsequent ipsilateral stroke. With the relatively small number of patients examined with both methods with subsequent strokes at follow-up (nine patients), however, we cannot conclude with any confidence that the count-based OEF technique is better than the quantitative OEF method (34).

One aspect of the count-based OEF method that may provide greater accuracy is the use of the normalizing factor. Quantitative OEF values can vary widely between subjects with normal cerebral hemodynamics but are relatively uniform within individual patients. For example, one subject may have a quantitative OEF of 0.40 in both hemispheres, and another may have a value of 0.30. These absolute values of OEF are within the range of normal. Because of this normal variation in absolute values, we use the hemispheric ratio of OEF to identify abnormally increased OEF. An individual with a mean OEF of 0.30 in the left middle cerebral arterial territory and 0.40 in the right would have a very abnormal OEF ratio: left-to-right ratio of 0.30/0.40 = 0.75, well outside of the normal range.

However, in patients with low absolute values of quantitative OEF, the left-to-right ratio is more likely to fall beyond the normal range than in patients with higher OEF values. For example, a mean OEF of 0.40 on the left and 0.42 on the right would be categorized as normal (ratio = 0.95) while a mean OEF of 0.20 on the left and 0.22 on the right (ratio = 0.909) would be categorized as abnormal. In other words, although the absolute difference in quantitative OEF between the hemispheres is the same in both patients, the relative difference is greater in the patient with lower absolute values. By normalizing the count-based OEF image to a whole-brain mean of 0.40 before calculating the hemispheric ratio, this potential bias in categorization of patients with low absolute values is avoided.

If a multicenter trial is organized to test the effect of surgical revascularization in selected patients with high OEF, the count-based method presented here would hold several advantages over the quantitative technique. First, it may be possible to successfully enroll more patients. It may not be possible or safe to place an arterial catheter in many patients with carotid occlusion. This occurred in six of the 13 patients in whom quantitative processing could not be completed. Also, technical problems may render the arterial time-activity curve data useless, as occurred in five of the remaining seven patients.

Second, processing the count-based images is less complicated. The processing of the PET images, arterial activity curves, and other necessary laboratory data (hematocrit values, etc) required to yield quantitative metabolic data is both time and labor intensive (17,27). Third, the count-based technique does not require the synthesis and administration of ^{15}O-labeled carbon monoxide for a cerebral blood volume scan. Finally, issues of standardization of PET methodology between institutions would be greatly simplified by using this count-based technique, as the software programs used for quantitative metabolic processing would need to be installed on different computer systems.

In summary, we have demonstrated that a count-based method of OEF measurement can be used to predict stroke in patients with symptomatic carotid occlusion. The sensitivity and specificity of this technique for the identification of patients at risk for stroke are comparable to those of the more complicated quantitative method. If a multicenter trial of surgical revascularization for patients with symptomatic carotid occlusion is organized, the count-based method of OEF measurement presented in this article should be used to select patients for surgery. The optimal threshold of the count-based OEF ratio used to select patients for surgery in such a trial will need to be determined through cost-effectiveness analysis.

References

1. Powers WJ, Press GA, Grubb RL Jr, Gado M, Raichle ME. The effect of hemodynamically significant carotid artery disease on the hemodynamic status of the cerebral circulation. Ann Intern Med 1987; 106: 27–35.
2. Baron JC, Bousser MG, Rey A, Guillard A, Comar D, Castaigne P. Reversal of focal "misery perfusion syndrome" by extra-intracranial artery bypass in hemodynamic cerebral ischemia: a case study with O-15 positron emission tomography. Stroke 1981; 12:454–459.
3. Powers WJ. Cerebral hemodynamics in ischemic cerebrovascular disease. Ann Neurol 1991; 29:231–240.
4. Barnett HJ. Hemodynamic cerebral ischemia: an appeal for systematic data gathering prior to a new EC/IC trial. Stroke 1997; 28:1857–1860.
5. Balow J, Alter M, Resch JA. Cerebral thromboembolism: a clinical appraisal of 100 cases. Neurology 1966; 16:559–564.
6. Pessin MS, Duncan GW, Mohr JP, Poskanzer DC. Clinical and angiographic features of carotid transient ischemic attacks. N Engl J Med 1977; 296:358–362.
7. Thiele BL, Young JV, Chikos PM, Hirsch JH, Strandness DE Jr. Correlation of arteriographic findings and symptoms in cerebrovascular disease. Neurology 1980; 30: 1041–1046.
8. Hankey GJ. Prognosis of symptomatic carotid artery occlusion. Cerebrovasc Dis 1991; 1:245–256.
9. Yonas H, Smith HA, Durham SR, Pentheny SL, Johnson DW. Increased stroke risk predicted by compromised cerebral blood flow reactivity. J Neurosurg 1993; 79:483–489.
10. Widder B, Kleiser B, Krapf H. Course of cerebrovascular reactivity in patients with carotid artery occlusions. Stroke 1994; 25:1963–1967.
11. Klijn CJ, Kappelle LJ, Tulleken CA, van Gijn J. Symptomatic carotid artery occlusion: a reappraisal of hemodynamic factors. Stroke 1997; 28:2084–2093.
12. Grubb RL Jr, Derdeyn CP, Fritsch SM, et al. Importance of hemodynamic factors in the prognosis of symptomatic carotid occlusion. JAMA 1998; 280:1055–1060.
13. Powers WJ, Martin WR, Herscovitch P, Raichle ME, Grubb RL Jr. Extracranial-intracranial bypass surgery: hemodynamic and metabolic effects. Neurology 1984; 34:1168–1174.
14. Samson Y, Baron JC, Bousser MG, et al. Effects of extra-intracranial arterial bypass on cerebral blood flow and oxygen metabolism in humans. Stroke 1985; 16:609–615.
15. Gibbs JM, Wise RJ, Thomas DJ, Mansfield AO, Russell RW. Cerebral haemodynamic changes after extracranial-intracranial bypass surgery. J Neurol Neurosurg Psychiatry 1987; 50:140–150.
16. Derdeyn CP, Powers WJ. Positron emission tomography: experimental and clinical applications. In: Batjer HH, ed. Cerebrovascular disease. Philadelphia, Pa: Lippincott-Raven, 1997; 239–253.
17. Mintun MA, Raichle ME, Martin WR, Herscovitch P. Brain oxygen utilization measured with O-15 radiotracers and positron emission tomography. J Nucl Med 1984; 25:177–187.
18. Baron JC, Steinling M, Tanaka T, Cavalheiro E, Sousaline F, Collard P. Quantitative measurement of CBF, oxygen extraction fraction (OEF) and CMRO2 with the O-15 continuous inhalation technique and positron emission tomography (PET): experimental evidence and normal values in man. J Cereb Blood Flow Metab 1981; 1(suppl 1):5–6.
19. Pantano P, Baron JC, Crouzel C, Collard P, Sirou P, Samson Y. The O-15 continuous-inhalation method: correction for intravascular signal using O-15 CO. Eur J Nucl Med 1985; 10:387–391.
20. Derdeyn CP, Yundt KD, Videen TO, Carpenter DA, Grubb RL Jr, Powers WJ. Increased oxygen extraction fraction is associated with prior ischemic events in patients with carotid occlusion. Stroke 1998; 29:754–758.
21. Raichle ME, Martin WR, Herscovitch P, Mintun MA, Markham J. Brain blood flow measured with intravenous H2(15)O. II. Implementation and validation. J Nucl Med 1985; 24:790–798.
22. Welch MJ, Ter-Pogossian MM. Preparation of short half-lived radioactive gases for medical studies. Radiat Res 1968; 36: 580–587.
23. Welch MJ, Lifton JF, Ter-Pogossian MM. The preparation of millicurie quantities of oxygen-15 labeled water. J Lab Clin Med 1969; 5:168–172.
24. Talairach J, Tournoux P. Co-planar stereotactic atlas of the human brain. New York, NY: Thieme Medical, 1988.
25. Grubb RL Jr, Raichle ME, Higgins CS, Eichling JO. Measurement of regional cerebral blood volume by emission tomography. Ann Neurol 1978; 4:322–328.
26. Herscovitch P, Markham J, Raichle ME. Brain blood flow measured with intravenous H2(15)O. I. Theory and error analysis. J Nucl Med 1983; 24:782–789.
27. Videen TO, Perlmutter JS, Herscovitch P, Raichle ME. Brain blood volume, blood flow, and oxygen utilization measured with O-15 radiotracers and positron emission tomography: revised metabolic computations. J Cereb Blood Flow Metab 1987; 7:513–516.
28. Fox PT, Perlmutter JS, Raichle ME. A stereotactic method of anatomical localization for positron emission tomography. J Comput Assist Tomogr 1985; 9:141–153.
29. Hanley JA, Lippman-Hand A. If nothing goes wrong, is everything all right? Interpreting zero numerators. JAMA 1983; 249: 1743–1745.
30. Altman DI, Lich LL, Powers WJ. Brief inhalation method to measure cerebral oxygen extraction fraction with PET: accuracy determination under pathologic conditions. J Nucl Med 1991; 32:1738–1741.
31. Jones T, Chesler DA, Ter-Pogossian MM. The continuous inhalation of oxygen-15 for assessing regional oxygen extraction in the brain of man. Br J Radiol 1976; 49:339–343.
32. Frackowiak RS, Lenzi GL, Jones T, Heather JD. Quantitative measurement of regional cerebral blood flow and oxygen metabolism in man using 15O and positron emission tomography: theory, procedure, and normal values. J Comput Assist Tomogr 1980; 4:727–736.
33. Lammertsma AA, Wise RJ, Heather JD, et al. Correction for the presence of intravascular oxygen-15 in the steady-state technique for measuring regional oxygen extraction ratio in the brain. II. Results in normal subjects and brain tumour and stroke patients. J Cereb Blood Flow Metab 1983; 3:425–431.
34. Hanley JA, McNeil BJ. The meaning and use of the area under a receiver operating characteristic (ROC) curve. Radiology 1982; 143:29–36.